Computer Simulations of Local Concentration Variations in Miscible Polymer Blends

Sumeet Salaniwal, Rama Kant,† Ralph H. Colby, and Sanat K. Kumar*,†

Department of Materials Science and Engineering, The Pennsylvania State University, University Park, Pennsylvania 16802

Received April 22, 2002

ABSTRACT: The dynamics of the two different components of thermodynamically miscible polymer blends can have very different temperature dependences ("thermorheologically complex") in some cases, while in others the two components behave more in agreement with intuition and have similar temperature dependences. The presence of spatial concentration variations over very local length scales (typically nanometers in size) caused by a combination of thermodynamic factors and chain connectivity effects is one explanation for thermorheological complexity. While several theories have been presented to rationalize this rich variety of rheological behavior, there remain lingering questions of the relative importance of system thermodynamics and chain connectivity effects in determining concentration variations over such small spatial domains. We critically investigate these issues using lattice Monte Carlo simulations on model binary blends. Our simulations show that the distribution of concentrations encountered within a specified control volume is indeed Gaussian with widths that are in excellent agreement with the predictions of mean-field theory. However, these distributions are centered at compositions that are significantly enriched due to chain connectivity effects. These results provide an excellent basis for the development of microscopic theories for the dynamics of polymer blends.

I. Introduction

Thermodynamically miscible polymer blends offer a relatively simple and cost-effective means of preparing useful materials with desired properties without the need to synthesize new polymers.[1] The viscoelastic properties of polymeric systems play an important role in their processing. For miscible polymer blends, available empiricisms can correlate properties such as the glass transition temperature and viscosity to the composition and the properties of the two pure components. However, lack of fundamental understanding of the principles controlling blend dynamics severely limits the predictive capabilities of such generalized correlations. Over the past few years, experiments on several miscible polymer blends provide evidence of thermorheological complexity,[2−6] which is defined as the failure of the empiricial time−temperature superposition (tTS) principle in describing system dynamics. Thus, it appears that the two components maintain their own dynamic identities even though the blend is thermodynamically miscible.

Fischer[7,8] was the first to propose a model which suggests that these unusual dynamics are driven by thermodynamic factors. These workers argued that thermally driven concentration fluctuations coupled to polymer chain connectivity effects[4,7−9] create a range of environments that are sampled by a monomer of interest. It is then postulated that the *segmental* dynamics of the chains are strongly influenced by the compositions experienced in a volume, termed the "cooperative volume", surrounding the monomer of interest.[10,11] Therefore, local dynamics are affected by thermodynamic factors (concentration variations) and by dynamic effects (which control the size of the "cooperative volume"). These concentration variations result in a distribution of segmental relaxation rates. While this combined approach apparently permits the modeling of the *segmental* dynamics of several miscible blends, a primary criticism is that concentration fluctuations at local length scales, that is ∼1 nm, cannot be altered significantly by the macroscopic thermodynamics of the blends. On this basis, Lodge and McLeish[12] have ignored the role of thermodynamic concentration fluctutations and have simply incorporated self-concentration effects at the level of the mean composition. That is, the mean effective composition experienced by a monomer is given by the equation

$$\bar{\phi}_{\mathrm{eff}} = \bar{\phi}_{\mathrm{self}} + (1 - \bar{\phi}_{\mathrm{self}})\bar{\phi} \tag{1}$$

where $\bar{\phi}$ is the macroscopic mean blend composition and $\bar{\phi}_{\mathrm{self}}$ is the mean value of self-concentrations experienced by the segment of interest.

Our objective in this paper is to investigate, at a molecular level, the role of chain connectivity effects and polymer−polymer intermolecular interaction on local concentration variations. Using lattice-based computer simulations of a binary polymer blend, we enumerate the distributions of concentrations sampled and separate them into self-concentration and intermolecular concentration fluctuation effects. Under the assumption that thermodynamic factors directly affect the local dynamics of polymer blends, the simulation results presented here provide incisive insights into the molecular origins of dynamic heterogeneity. Our results clearly show that thermodynamic interactions play a critical role in determining the width of the distribution of concentrations sampled by a monomer of interest. Further, these widths are *quantitatively* modeled by the mean-field theory resulting from the random phase approximation (RPA), showing that these macroscopic ideas are surprisingly valid even at length scales of a few Kuhn segments. Finally, we find that the width of the distribution of concentrations sampled due to self-

† Current address: Department of Chemical Engineering, Rensselaer Polytechnic Institute, Troy, NY.

10.1021/ma020624k CCC: $22.00
Published on Web 10/19/2002

concentration effects is comparable to that of the intermolecular effects (driven by thermodynamics). These facts strongly argue in favor of using distributions of concentrations driven by thermodynamics and chain connectivity, not simply the mean values that may be obtained for each of these effects, in determining the environment sampled by a monomer of interest.

II. Simulation Model

A cubic lattice model, similar in spirit to the Flory–Huggins model, is employed in this study. We simulated lattices of size 50^3 with a cordination number of $z = 6$ and utilized periodic boundary conditions in all three directions. The system is comprised of polymer chains and holes, and to mimic a melt, we consider a relatively high polymer volume fraction, $\phi = 1 - \phi_v = 0.8$. Each polymer chain is represented as a fully flexible string of beads connected by bonds of fixed length. Each site is occupied, at most, by one monomer. For simplicity, we have considered a fully symmetric polymer blend.[13,14] That is, we consider equimolar blends where each component is monodisperse and both components are of the same chain length ($N_A = N_B = N$). Interbead interactions between chain segments of the same type are assumed to be isomorphic to those between a segment and a hole, or between two holes, that is, $\epsilon_{AA} = \epsilon_{BB} = 0$. The interaction energy between dissimilar beads, ϵ_{AB}, is then the only nonzero energy in the simulations. We define the *bare* χ parameter by the equation

$$\chi = \frac{(z-2)\epsilon_{AB}}{k_B T}(1-\phi_v)^2 \tag{2}$$

which represents the inverse of the reduced temperature in the system. Note that this definition of χ is somewhat different from the Flory prescription,[15] and we justify this form as follows: the factor of $(z - 2)$ arises since each internal monomer has two monomers of the same type bonded to it. Thus, the number of lattice sites available for intermolecular interactions is reduced due to chain connectivity effects. Such ideas are motivated directly by the work of Guggenheim.[16] Similarly, the factor of $(1 - \phi_v)^2$ accounts for the fact that Flory theory is relevant to an incompressible mixture, while our mixture is compressible. At a mean-field level the number of molecule–molecule contacts is reduced in a compressible mixture by precisely a factor of $(1 - \phi_v)^2$. Here we report results for two different chain lengths, $N = 100$ and 500. Simulation results for $\chi = 0$ (athermal) and -0.05 (strongly miscible) systems for $N = 100$ are presented, while only results for $\chi = 0$ are presented for the $N = 500$ system.

While the bare χ parameter is defined in terms of energetic interactions alone, the effective interaction parameter, χ_{eff}, which needs to be employed in the Flory–Huggins free energy of mixing to properly describe system thermodynamics would also include entropic contributions.[13,17] We have calculated the chemical potential changes on mixing for both components of all the blends considered so as to evaluate these entropic terms but find that the uncertainties in these results are large enough that we cannot definitively determine the relevant χ_{eff}. Consequently, we shall use $\chi_{eff} \equiv \chi$.

It is important to ensure that the simulations equilibrate before their results on concentration fluctuations can be considered. The desired blend density within the simulation cell was achieved by packing chains on the lattice in a crystalline motif. Subsequently, a mix of $\sim(2-4) \times 10^{10}$ Monte Carlo moves, that is, reptation (30%), bond flip (50%), and chain regrowth (20%), was employed for equilibration. We monitored the normalized end-to-end vector autocorrelation function, a_t, to examine the equilibration of the systems:

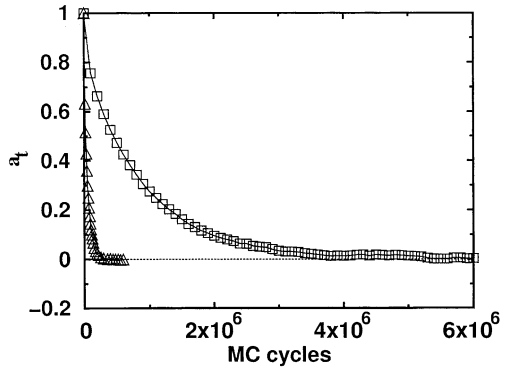

Figure 1. End-to-end vector autocorrelation function for polymer blends of $N = 100$ (triangles) and $N = 500$ (squares). $\chi = 0$ in both cases.

$$a_t \equiv \frac{\langle \vec{r}(t)\cdot\vec{r}(0)\rangle}{|\vec{r}(0)|^2} \tag{3}$$

where $\vec{r}(0)$ and $\vec{r}(t)$ denote the end-to-end vector of polymer chains at some reference time ($t = 0$) and at a later time t. Figure 1 shows the end-to-end vector autocorrelation function for blend systems of $N = 100$ and $N = 500$ ($\chi = 0$ in both cases). As seen in the figure, for both systems, the autocorrelation function decays from unity at $t = 0$ to zero at long times. As expected, a_t for the $N = 500$ blend decays much slower than that for the $N = 100$ blend. We have also conducted a few simulations with a "chain swap" move, where the position of a chain of type A is exchanged with that of a chain of type B. This move is incorporated to ensure that concentrations are also equalized in these simulations. Since we found no difference in results with or without the swap move, we conclude that it is sufficient to monitor the end-to-end distance autocorrelation function to determine whether the simulations are properly equilibrated.

In our simulations we primarily focus on calculating the distribution of concentrations around either a test lattice site or a test monomer. In cases where the volume is centered around a test monomer, we break the concentrations down into "intramolecular", "intermolecular", and total compositions. (More details are presented below in the beginning of the Results section.) These concentrations are studied for different values of the size of the "cooperative volume". Note that we do not examine the pair distribution functions since these are strongly affected by the structure of the lattice (and hence the discrete values of interbead separation), especially at the small distances of interest. Similarly, we do not study the behavior of the scattering function (the Fourier transform of the pair distribution function) since this behavior has been extensively studied and compared to theoretical predictions elsewhere.[13,14]

III. Results

When one measures the distribution of concentrations within a given volume, it is important to decide how to

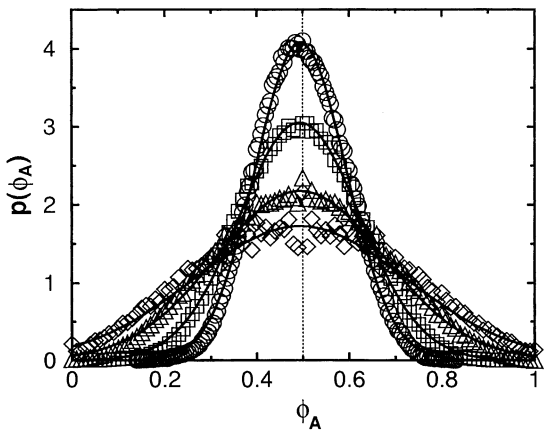

Figure 2. Normalized probability density distribution of ϕ_A for the $N = 500$, $\chi = 0$ blend surrounding a randomly chosen site. The symbols represent different sizes of spherical volumes: diamonds for $r_a = \sqrt{10}$; triangles for $r_a = \sqrt{20}$; squares for $r_a = \sqrt{50}$; circles for $r_a = \sqrt{100}$. Solid lines are Gaussian function fits to the simulation data (eq 10).

select the lattice site that will serve as the origin for the cooperative volume. Two possible choices exist. First, we can select a lattice site at random and, irrespective of whether it is a chain monomer or a hole, compute the volume fractions of the two polymers in the volume of interest. In the second case, an A monomer is selected at random, and the volume fraction of the two polymers in the volume surrounding this chosen monomer is examined. These two distributions are of particular interest since they provide complementary information which can be compared to existing theory. The first expression, which computes the fluctuation at any arbitrarily chosen lattice site, can be compared to theoretical expressions such as the random phase approximation (see eq 11 of the Appendix). This distribution, however, would not be able to distinguish the importance of chain connectivity effects in a 50:50 blend since an arbitrarily selected lattice site could either be an A segment or a B segment with equal probability: if an A site were selected, then the intramolecular A effect would skew the computed composition to the A-rich side. This effect, however, would be exactly compensated by the situation where a B segment was selected. In contrast, the dynamics of miscible blends would necessarily be governed by the second distribution, which describes the distributions of concentrations viewed by a segment of interest. In this case both thermodynamic fluctuations and chain connectivity effects are expected to be important, and it is unclear whether existing theory can describe these effects successfully. Below, we will consider both of these distributions and examine the fidelity with which theory describes them. The theoretical ideas that describe these distributions are presented in the Appendix.

A. Distributions about Randomly Selected Lattice Sites. We randomly choose lattice sites, examine spherical volumes of radius r_a, and tabulate the normalized composition of A sites in each:

$$\phi_A = \frac{n_A}{n_A + n_B} \tag{4}$$

where n_A and n_B are the number of A beads and B beads within the control volume. Figure 2 presents the normalized probability density distribution $p(\phi_A)$ for the

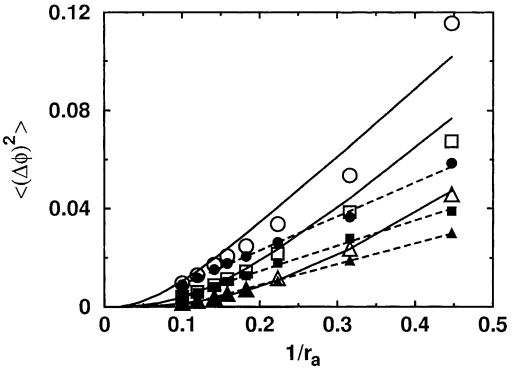

Figure 3. Comparison between the simulation data for $\langle(\Delta\phi_A)^2\rangle$ (hollow symbols), $\langle(\Delta\phi_{eff})^2\rangle$ [ϕ_{eff} is defined in eq 7] (filled symbols), and RPA predictions for various blend systems. The symbols represent different chain lengths and interaction parameters: circles for $N = 500$, $\chi = 0$; squares for $N = 100$, $\chi = 0$; and triangles for $N = 100$, $\chi \sim -0.05$. Solid lines are RPA predictions (eq 11). Dashed lines are guides to the eye.

polymer blend with $N = 500$ and $\chi = 0$. The figure shows that, as expected,[18] $p(\phi_A)$ can be accurately described by a Gaussian distribution for all r_a's considered. The Gaussian distribution fits are centered at the mean blend composition. Results for the $N = 100$ blends, with two different χ values (not shown), are also accurately described by Gaussian distributions centered at the mean blend composition. Figure 2 also shows that for the smallest control volume ($r_a = \sqrt{10}$) there is an equal probability of finding control volumes that are devoid of A beads ($\phi_A = 0$) or B beads ($\phi_A = 1$).

Figure 3 presents the comparison between the computed widths of the distributions, $\langle(\Delta\phi_A)^2\rangle$, and those predicted by the RPA model following eq 11. We first make a few qualitative observations. A change in chain length from $N = 500$ to $N = 100$ for the $\chi = 0$ system results in a noticeable decrease in the width of the concentration profiles. Similar strong effects are observed on $\langle(\Delta\phi_A)^2\rangle$ when χ is changed from 0 to -0.05 even for volumes that are only twice as big as a Kuhn segment in radius. (For these lattice chains a Kuhn segment is ~1.3 lattice units long.) These results strongly argue that system thermodynamics play a decisive role in determining the concentration fluctuations even for cooperative volumes which have been postulated as being small enough to affect segmental dynamics. It is also clear that, for all the blend systems considered, the agreement between the theoretical predictions and the simulations is excellent.[19]

B. Distributions about Randomly Selected Polymer Segments of One Type. *1. Intermolecular Fluctuations.* We define the *intermolecular* volume fraction of A−A contacts, ϕ_m, in a sphere of radius r_a lattice units as

$$\phi_m = \frac{n_{A,inter}}{n_{A,inter} + n_B} \tag{5}$$

where $n_{A,\,inter}$ is the number of A beads within the control volume that belong to polymer chains other than the one that has a central A bead. n_B is the number of B beads surrounding the reference bead within the control volume. The particular normalization employed in the definition of the intermolecular composition ensures that ϕ_m will range from 0 to 1. Figure 4 presents the effect of r_a on the probability density distribution, $p(\phi_m)$, for the $N = 100$ blends with two different χ values.

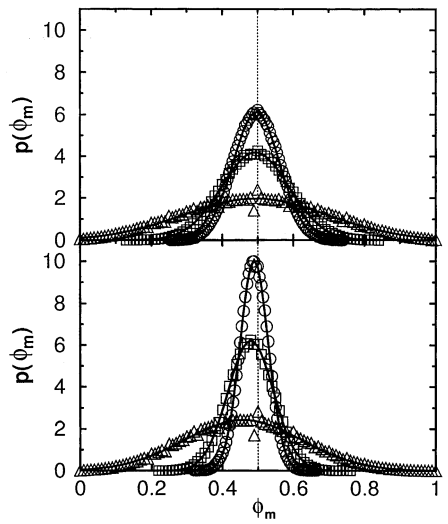

Figure 4. Normalized probability density distribution of the intermolecular volume fraction, ϕ_m, for the $N = 100$, $\chi = 0$ blend system (top) and $\chi \sim -0.05$ (bottom). The symbols represent different control volume sizes: triangles for $r_a = \sqrt{10}$; squares for $r_a = \sqrt{50}$; and circles for $r_a = \sqrt{100}$. Solid lines are Gaussian function fits to the simulation data.

The solid curves are the Gaussian function fits to the simulation data. The following interesting observations can be made from this figure.

(i) As expected for a 50:50 binary blend with $N_A = N_B$ and $\chi = 0$, the average value of ϕ_m corresponds to the macroscopic mean blend composition for all control volume sizes. $p(\phi_m)$ displays a Gaussian distribution.

(ii) As the size of the control volume decreases, the density distribution becomes broader. For the smallest control volume considered, that is, $r_a = \sqrt{10}$, $p(\phi_m)$ is nonzero at $\phi_m = 0$ and $\phi_m = 1$. As expected, the central A bead experiences a wider range of local compositions as the size of the control volume decreases.

(iii) Favorable thermodynamic interactions narrow the distribution of concentration fluctuations. While this effect is most pronounced for the large cooperative volumes, it still persists for the smallest r_a values studied.

(iv) For the $\chi = 0$ blend, the peak concentration always corresponds to the mean blend composition, while for the $\chi \sim -0.05$ blend it is seen that the peak concentration is depleted in A segments. This trend, which decreases with increasing r_a values, stresses the importance of strong attractive interactions in this blend.

We have fit the distributions of ϕ_m to Gaussian functions and thus have obtained estimates of both the mean composition and the variance which is assigned to the quantity $\langle(\Delta\phi_m)^2\rangle$. Figure 5 presents the simulation results for $\langle(\Delta\phi_m)^2\rangle$ for different blend systems. For all the blends shown, $\langle(\Delta\phi_m)^2\rangle$ increases monotonically as the size of the control volume is decreased. For a given size, $\langle(\Delta\phi_m)^2\rangle$ decreases as the chain length is reduced or polymer−polymer intermolecular interactions become attractive, as expected. The effect is quite pronounced even for small control volumes. The lines in this figure, which result from the application of eq 11, are in good agreement with the simulation results, thus stressing that this simple mean-field picture accurately captures the role of polymer chain length and interactions on system thermodynamics. It is surprising that the RPA predictions continue to give a good

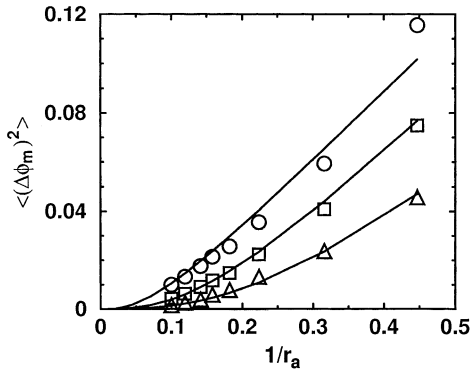

Figure 5. Comparison between simulation data for the mean-square variance of intermolecular volume fraction, $\langle(\Delta\phi_m)^2\rangle$, and RPA predictions for the three blends studied: circles for $N = 500$, $\chi = 0$; squares for $N = 100$, $\chi = 0$; and triangles for $N = 100$, $\chi \sim -0.05$. Solid lines are the RPA predictions (eq 11).

description of concentration fluctuations even for control volumes as small as $r_a = \sqrt{5}$, where Gaussian statistics no longer describe chain conformations.

2. Chain Connectivity Effects. As mentioned earlier, chain connectivity effects give rise to the self-concentration which is defined as the *intrachain* contribution to the local composition. Prior research efforts[5,12] have identified the role of chain connectivity effects in biasing the local composition toward the component whose segment is at the center of the control volume. These effects were incorporated in a mean sense and resulted in dynamic asymmetry in these systems. However, these past works provide little insight into the distribution of self-concentration and whether it is reasonable to approximate this distribution through its mean value. To quantify chain connectivity effects, we estimate the self-concentration (ϕ_{self}) from our simulations as

$$\phi_{self} = \frac{n_{A,intra}}{n_{A,intra} + n_{A,inter} + n_B} \tag{6}$$

where $n_{A,intra}$ are contributions from the chain to which the central A monomer belongs. Note that these estimates only account for the single-pass length (SPL); that is, they begin with a monomer at the center and monitor the number of chain monomers before the chain first exits the control volume. A similar calculation is made for the other walk that originates from the origin. In this calculation we ignore any long-range self-concentration effects. Estimates of $p(\phi_{self})$ are also obtained from our theoretical model (eq 19 in the Appendix). Figure 6 presents the simulation data and theoretical predictions of eq 19 for $p(\phi_{self})$ based on the single-pass length for the athermal blend system with $N = 500$. For all r_a values considered, the theoretical predictions of ϕ_{self} are in good agreement with the simulations. Interestingly, the agreement between the two approaches improves considerably as the size of the control volume decreases. Note that $p(\phi_{self})$ cannot be described by a Gaussian distribution. The width of the probability distribution increases as the size of the control volume decreases, which is consistent with the fact that chain connectivity effects become more important for smaller control volumes. Prior estimates of chain connectivity effects by Lodge[12] and Kornfield[5] utilized average values of the self-concentration ($\bar{\phi}_{self}$) instead of the distribution of self-concentrations shown in Figure 6. These mean

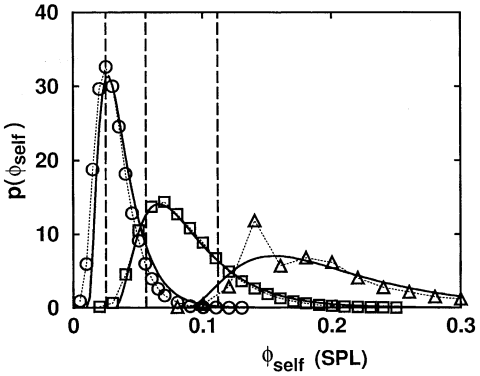

Figure 6. Normalized probability density distribution of the self-concentration for the polymer blend with $N = 500$ and $\chi = 0$ for different control volume sizes: triangles for $r_a = \sqrt{5}$; squares for $r_a = \sqrt{20}$; and circles for $r_a = \sqrt{100}$. Solid lines are predictions of eq 19. The vertical lines are mean values of the self-concentration as suggested by refs 5 and 12.

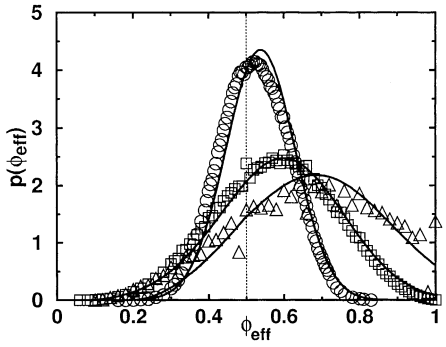

Figure 7. Normalized probability density distribution of ϕ_{eff} for the $N = 500$, $\chi = 0$ blend system. The symbols represent different sizes of control volumes: triangles for $r_a = \sqrt{5}$; squares for $r_a = \sqrt{20}$; and circles for $r_a = \sqrt{100}$. Solid lines are predictions of eq 20.

estimates, which are also shown in the figure, closely approximate the position of the maximum probability at least for the larger r_a values. However, an important point is that, for the small sizes of cooperative volumes suggested as appropriate for modeling blend dynamics, ϕ_{self} is very broadly distributed. Ignoring this distribution and focusing on its mean value is hence a crude approximation, which cannot be justified on the basis of our simulation data. We stress that both the intermolecular and intramolecular contributions to concentration fluctuations must be considered at the level of distributions if an appropriate description of blend dynamics is to be achieved self-consistently.

3. Effective Local Composition. A direct consequence of chain connectivity effects is that for miscible polymer blends the effective local composition (ϕ_{eff}) that a polymer segment at the center of a given control volume experiences is biased toward blend compositions enriched in its own type. To clarify, this arises since the effective composition counts contributions from both intermolecular and intramolecular fluctuations. Theoretically, ϕ_{eff} is estimated by the equation

$$\phi_{eff} = \phi_{self} + (1 - \phi_{self})\phi_m \tag{7}$$

where ϕ_m is the intermolecular composition encountered in the volume, and it is assumed that holes are randomly distributed. This equation, which permits the evaluation of the distribution of ϕ_{eff} based on intramolecular and intermolecular contributions to local composition, is a generalization of eq 1. ϕ_{eff} can be directly calculated from our simulation data by the equation

$$\phi_{eff} = \frac{n_A}{n_A + n_B} \tag{8}$$

where n_A and n_B are respectively the number of A and B monomers in the volume of interest. Note that, while ϕ_{eff} and ϕ_A (eq 4) are formally defined by the same expression, the former quantity is only defined for volumes with an A bead at the center. In contrast, ϕ_A is defined with *any* randomly selected lattice site, be it an A, a B, or a hole. Figure 7 presents $p(\phi_{eff})$ as estimated directly from the simulations and from the theoretical model (eq 20) based on the knowledge of the distributions of the self- and intermolecular volume fractions in a given volume. As expected, both the simulations and theory predict that $p(\phi_{eff})$ will be approximately Gaussian, but centered at compositions greater than the mean blend composition for all control volume sizes considered. As the size of the control volume increases, $\bar{\phi}_{eff}$ approaches the mean blend composition. It is somewhat surprising that, although we have very good predictive capability for ϕ_{self} and ϕ_m, the predictions for ϕ_{eff} are not perfect, especially for large r_a values. It is possible that the error in accounting for the intramolecular contributions at the level of the single passage length excludes any long-range contribution to the self-concentration. We have attempted to rectify this problem by including the total passage length (TPL) for a Brownian walk in a sphere of radius r_a. Note that, by its construction, the literature results for the TPL are relevant only to chains of infinite length. As a consequence, we have found that theoretical results using this TPL expression for self-concentrations only work well for small r_a (typically less than $\sqrt{10}$), where the infinite chain length of the theoretical results are not relevant. For larger r_a values this expression results in the theory overpredicting the importance of self-concentration, thus causing the predicted ϕ_{eff} peak to be too rich in the A component. We therefore have two qualitatively correct, but quantitatively imperfect, means of calculating the effective concentration experienced by a test segment. Since both approaches work to similar accuracy for the cooperative volume sizes of interest, that is, $3 \leq r_a \leq 20$, we recommend the simpler SPL approach.

Figure 3 also includes the simulation values of $\langle(\Delta\phi_{eff})^2\rangle$, the widths of the distribution. It is clear that the width of $p(\phi_{eff})$ density distribution is significantly narrowed relative to the unbiased distribution ($p(\phi_A)$), particularly for short length scales, due to connectivity effects. The important point included in Figure 7 is that our models for chain connectivity and intermolecular concentration fluctuations directly permit us to obtain the distributions of effective concentrations that are seen by a segment of interest. Since this information is critical to the evaluation of the dynamics of the two components of polymer blends, we now have all of the necessary pieces to make serious inroads to the calculation of these responses.

IV. Discussion

A few points regarding past work need to be stressed here. First, in previous work we have replaced eq 11 by its zero wavevector limit,[9] for the sake of simplicity.

$$\langle(\Delta\phi)^2\rangle = \frac{S(0)}{r_a^3} \tag{9}$$

We have compared the accuracy of this approximation in describing the simulation data but find that, while it is qualitatively correct in reproducing the r_a dependence of $\langle(\Delta\phi)^2\rangle$, it is quantitatively incorrect even in the case of the $\chi = 0$ blend. Equation 9 overestimates $\langle(\Delta\phi)^2\rangle$ by as much as 1 order of magnitude (results not shown). Consequently, if a quantitative understanding of the importance of concentration fluctuations is required, then this zero wavevector limit must not be employed. Instead, eq 11 provides a nearly quantitative description of $\langle(\Delta\phi)^2\rangle$.

It is also important to understand the reasons behind the qualitative difference between the distribution of concentrations based on the two possible choices of reference lattice site. By randomly selecting a reference lattice site irrespective of whether it is a chain monomer (A or B) or a hole, the chain connectivity effects are exactly eliminated in a 50:50 blend. Since only the thermodynamic contributions remain in this case, the simulation results are in excellent agreement with the RPA predictions. In contrast, by randomly selecting an A monomer as the reference lattice site, a lower limit is set on the range of local composition of A monomers. This effect is more pronounced at small control volumes because of the large contribution from self-concentration at such short length scales (see Figure 6). Consequently, the width of the density distribution in the second case is significantly reduced.

The most important observation here is that both the intermolecular composition and self-connectivity effects are broadly distributed, especially at the small r_a values which have been proposed as being relevant to segmental dynamics.[12] Since different compositions can have very different T_g's, and hence relaxation times, these distributions can have a large impact on the distribution of relaxation times of experimental blends which display thermorheological complexity. We therefore stress that for a self-consistent implementation of this theory both the intermolecular and connectivity effects be considered not through their mean values, but rather through their distributions. Since theory provides a reasonable description of these distributions, we shall perform these calculations, and contrast them to calculations that employ only mean values of compositions,[12] in a future paper.

V. Conclusions

We have utilized Monte Carlo simulations to critically evaluate the magnitude of concentration fluctuations, both driven by chain connectivity effects and thermodynamic fluctuations, in small cooperative volumes which are relevant to predicting the dynamics of miscible polymer blends. Chain connectivity effects can lead to very large concentration variations, but in a manner that can be understood from concepts of the "first passage time" relevant to Brownian diffusion. The thermodynamically driven concentration fluctuations are strongly affected by system thermodynamics even for very small cooperative volumes, and we find that these effects can be captured accurately by a simple application of the RPA model developed to describe the long wavelength properties of polymer blends. In summary, these results strongly suggest that the distributions of concentration experienced by a polymer segment can be anticipated by available concepts in the literature and also that these distributions are generally so broad that they cannot be treated through the use of mean values alone. These ideas are expected to provide a much improved handle on the dynamics of polymer blends.

Acknowledgment. We thank the National Science Foundation (CTS-9975625 and DMR-9977928) for financial support. We also thank Mark Ediger for providing the motivation for this research and for giving detailed and insightful comments on a draft of this manuscript.

Appendix. Theoretical Predictions for Self- and Intermolecular Fluctuations

Here we briefly describe ideas from the literature for evaluating the distribution of local concentration variations due to thermodynamic factors and due to chain connectivity effects. These ideas are useful for interpreting our simulation results.

A. Thermodynamically Driven Fluctuations. Statistical mechanics driven spontaneous concentration fluctuations result in a Gaussian distribution of local compositions within the blend:[7]

$$P(\phi) \propto \exp\left[-\frac{(\phi - \bar{\phi})^2}{2\langle(\Delta\phi)^2\rangle}\right] \tag{10}$$

where $\bar{\phi}$ denotes the bulk blend composition, ϕ is the local composition sampled, and $\langle(\Delta\phi)^2\rangle$ is the mean-squared concentration fluctuation within the microscopic control volume V surrounding the polymer segment. $\langle(\Delta\phi)^2\rangle$ is directly related to the thermodynamics of the polymer blend and the cooperative volume of relaxation by[7,20]

$$\langle(\Delta\phi)^2\rangle = \frac{b^3}{2\pi^2}\int_0^\infty S(q)(qF_q)^2\,dq \tag{11}$$

where $S(q)$ is the static structure factor, F_q denotes the form factor of the cooperative volume, and b^3 is the volume of a Kuhn segment. For a spherical cooperative volume with radius r_a ($\sim V^{1/3}$), the F_q is given by[7]

$$qF_q = \frac{1}{r_a}\left[\frac{3(\sin qr_a - qr_a\cos qr_a)}{(qr_a)^2}\right] \tag{12}$$

For an incompressible binary polymer blend, the random phase approximation (RPA) provides an estimate of $S(q)$[21]

$$\frac{1}{S(q)} = \frac{1}{\phi_A N_A g_D^A(q)} + \frac{1}{\phi_B N_B g_D^B(q)} - 2\chi \tag{13}$$

where ϕ_i and N_i denote the volume fraction and polymer chain length for species i. The Debye function, $g_D(q)$, is[21]

$$g_D(q) = \frac{2}{q^4 R_g^4}[e^{-q^2R_g^2} + q^2R_g^2 - 1] \tag{14}$$

where R_g is the radius of gyration of the polymer chain.

B. Chain Connectivity Effects. We now briefly describe the formalism for estimating the probability density distribution of self-concentration, $p(\phi_{self})$, within

a spherical control volume centered on the monomer of interest. The basic assumption in this model is that the polymer chain behaves as a *random coil* and hence obeys Gaussian chain statistics. The approach adopted here for estimating $p(\phi_{self})$ involves calculating the joint probability density function of two independent random walks, each of which originates at the center of the spherical control volume of radius r_a and passes through its surface. This approach is analogous to the analysis proposed by Ciesielski and Taylor[22] for calculating the single-passage time for a Brownian walk originating at the center of a spherical volume and passing through its surface. To make connection between the Brownian results and the single-pass length (SPL) of a polymer chain, it is convenient to define the quantity $P(n'|r_a)$:

$$P(n'|r_a) = \int_{n'}^{\infty} \not{p}(x|r_a)\, dx \tag{15}$$

Here n' is the number of monomers in a polymer chain random walk which begins at the origin of a spherical volume of radius r_a and ends at its surface. $\not{p}(x|r_a)$ denotes the probability density of finding a walk beginning at the center of the volume and reaching the surface after exactly x steps. The literature yields an expression for the $P(n'|r_a)$ for the SPL:[22]

$$P(n'|r_a) = 2\sum_{r=1}^{\infty}(-1)^{r-1} \exp(-n'b^2q_r^2/6r_a^2) \tag{16}$$

where q_r are the positive roots of the Bessel functions $J_{1/2}(z)$ and b is the Kuhn segment length of the chains. The probability density of finding a walk of length n_s which traverses the volume of interest while placing a monomer at the center of the volume is

$$p^{\star}(n_s|r_a) = \int_0^{n_s} \not{p}(n'|r_a)\not{p}(n_s - n'|r_a)\, dn' \tag{17}$$

where n_s is the total number of monomers constituting the SPL. It is important to note that eq 17 includes all contributions arising from the two independent random walks which constitute the SPL of n_s segments. Since Brownian motion is used to describe the SPL, contributions due to the overlap of the polymer segments are automatically included in the analysis. Finally, for polymer chains with segment volumes much smaller than the spherical control volume ($b^3/r_a^3 \ll 1$), the corrected joint probability density function is given by

$$\rho(n_s) = \begin{cases} 0 & n_s < n_{min} \\ p^{\star}(n_s - n_{min}|r_a) & n_{min} \le n_s \le n_{max} \end{cases}$$

$$p(n_s) = \rho(n_s)/\int_0^{n_{max}} \rho(x)\, dx \tag{18}$$

where n_{min} denotes the minimum number of Kuhn segments needed for the shortest single-pass length ($n_{min} = r_a/b$) and n_{max} denotes the maximum number of Kuhn segments that can be packed within the spherical volume ($n_{max} \sim r_a^3/b^3$). The volume fraction is defined as $\phi_{self} = n_s/n_{max}$. Figure 8 shows the comparison between the simulation estimates of $p(\phi_{self})$ and those obtained based on eq 17 for a control volume of size $r_a = \sqrt{20}$. As seen in the figure, eq 17 (long-dashed line) significantly overestimates the maximum in the distribution of self-concentration. Similar results are found

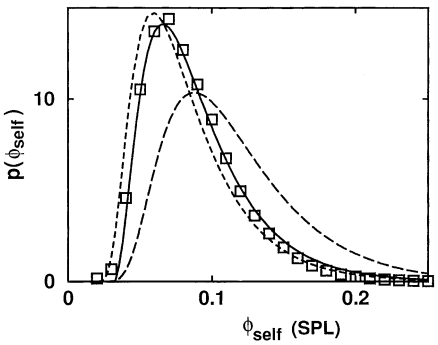

Figure 8. Normalized probability density distribution of the self-concentration for the polymer blend with $N = 500$ and $\chi = 0$ for a control volume of size $r_a = \sqrt{20}$. The points are simulation results and the long dashed line is the prediction of eq 17, while the short dashed line and solid line are predictions of the first and both terms of eq 19, respectively.

for all the control volume sizes considered in this study. The disagreement between the theory and simulations can be attributed to the fact that excluded-volume chains are considered in the simulations, while eq 17 is derived for chains with no excluded volume. These failures of the theory can be seen and remedied by writing eq 17 as a Taylor series expansion:

$$p^{\star}(n_s|r_a) \approx \not{p}(n_s|r_a)[1 - P(n_s|r_a)] - \frac{d\not{p}(n_s|r_a)}{dn_s}\int_0^{n_s} \not{p}(n'|r_a)n'\, dn' \tag{19}$$

where only the first two terms of the expansion, which account for the nonoverlapping contribution to SPL, have been retained. Figure 8 also shows the theoretical predictions based on eq 19. The dashed line is the prediction using only the first term in eq 19 while the solid line is the prediction using both the terms. Both the predictions based on eq 19 provide a significantly better description of the simulation data than eq 17, thus reiterating that the failure of eq 17 arises from the inclusion of overlapped configurations that would be reflected in higher-order terms in eq 19.

C. Net Local Composition. The probability distribution for the effective local composition can be calculated by

$$p(\phi_{eff}) = \int_0^{\phi_{eff}} p(\phi_{self})\, p(\phi)\, d\phi_{self} \tag{20}$$

where this equation sums the consequences of thermodynamics and chain connectivity effects. Clearly this equation is a convolution of both the intramolecular and intermolecular effects, where ϕ_{self} and ϕ sum to yield ϕ_{eff} following eq 7.

References and Notes

(1) Folkes, M. J.; Hope, P. S. *Polymer Blends and Alloys;* Blackie Academic and Professional: Glasgow, 1993.
(2) Colby, R. H. *Polymer* **1989**, *30*, 1275.
(3) Zawada, J. A.; Ylitalo, C. M.; Fuller, G. G.; Colby, R. H.; Long, T. E. *Macromolecules* **1992**, *25*, 2896.
(4) Roland, C. M.; Ngai, K. L. *Macromolecules* **1991**, *24*, 2261.
(5) Chung, G.-C.; Kornfield, J. A.; Smith, S. D. *Macromolecules* **1994**, *27*, 964.
(6) Chung, G.-C.; Kornfield, J. A.; Smith, S. D. *Macromolecules* **1994**, *27*, 5729.
(7) Zetsche, A.; Fischer, E. W. *Acta Polym.* **1994**, *45*, 168.
(8) Katana, G.; Fischer, E. W.; Hack, T.; Abetz, V.; Kremer, F. *Macromolecules* **1995**, *28*, 2714.

(9) Kumar, S. K.; Colby, R. H.; Anastasiadis, S. H.; Fytas, G. *J. Chem. Phys.* **1996**, *105*, 3777.
(10) Donth, E. *Polym. Commun.* **1990**, *31*, 139.
(11) Colby, R. H. *Phys. Rev. E* **2000**, *61*, 1783.
(12) Lodge, T. P.; McLeish, T. C. B. *Macromolecules* **2000**, *33*, 5278.
(13) Sariban, A.; Binder, K. *Macromolecules* **1988**, *21*, 711.
(14) Sariban, A.; Binder, K. *J. Chem. Phys.* **1987**, *86*, 5859.
(15) Flory, P. J. *Principles of Polymer Chemistry;* Cornell University Press: Ithaca, NY, 1953.
(16) Guggenheim, E. A. *Liquids and Liquid Mixtures;* Clarendon: New York, 1966.
(17) Kumar, S. K. *Macromolecules* **1994**, *27*, 260.
(18) Chandler, D. *Phys. Rev. E* **1993**, *48*, 2898.
(19) The RPA model relates to an incompressible polymer melt, while our simulations deal with a compressible blend. We can extend our calculations to incorporate the compressibility of the blend, but it is unclear which derivative needs to be calculated. Since our blends are considered at constant density, i.e., constant ϕ_v, a reasonable derivative is to calculate $\partial^2(\Delta G)/\partial\phi_A^2$ to keep in spirit with the Flory calculation. This would only alter our results by a factor of ϕ, i.e., less that 20%. To within these uncertainties in analysis, the incompressible RPA model describes the simulation results accurately.
(20) Ruland, W. *Prog. Colloid Polym. Sci.* **1975**, *57*, 192.
(21) deGennes, P. G. *Scaling Concepts in Polymer Physics;* Cornell University Press: Ithaca, NY, 1979.
(22) Ciesielski, Z.; Taylor, S. J. *Trans. Am. Math. Soc.* **1962**, *103*, 434.

MA020624K